On-Line Tracking of Six Orbital Elements of a Thrust Maneuvering Space Vehicle

KAY YONG*
Computer Sciences Corporation, Silver Springs, Md.
AND
CHI-NENG SHEN†
Rensselaer Polytechnic Institute, Troy, N.Y.

A set of discrete nonlinear measurement and dynamical equations has been established employing the position and angular momentum vectors from the tracking station to a maneuvering vehicle in three-dimensional space. Based upon the second order Taylor's expansion of nonlinear functions, a discrete first and second-order filtering relation is developed. A rapid estimation scheme is introduced to compute on line the correct state error covariance matrix for the six orbital elements at the instant of thrusting. Simulation results show significant improvement by adopting these schemes for orbital state estimation, compared to the unforced quasilinear filter.

Introduction

THE problem of satellite tracking by a ground radar employing the Kalman filtering technique has drawn considerable attention in recent years.[1-3] However, very few papers have discussed the problem of on-line tracking of a space vehicle when it is subjected to some unknown impulsive thrusting maneuverability. Shen[4] investigated a reduced problem considering the motion of the vehicle constrained to a plane. Three linear measurement equations containing the radial distance, velocity and acceleration of the vehicle were developed to estimate three state variables described by a Markov linear dynamical process. However, it is unrealistic to restrict the problem such that the motion of the vehicle and the tracking station are always lying in the same plane. The purpose of this paper is to develop a set of general discrete nonlinear measurement and dynamical equations such that the maneuverable vehicle can be tracked on-line in a three-dimensional space by one or several ground radar tracking stations.

The extended Kalman filtering technique (or quasilinear filter) has been developed to handle the state estimation of nonlinear systems.[5,6] However, if the interval between measurement stages becomes large, unsatisfactory state estimation results when employing the quasilinear filtering technique. Athans, Wishner and Bertolini[7] derived a second-order filtering relation for a continuous time nonlinear system with discrete noisy measurements. This scheme provides much better state estimation than the first-order quasilinear filtering relation. The problem discussed here contains a nonlinear discrete dynamical system as well as discrete noisy measurement equations. Thus, a second-order estimation relation must be derived for the nonlinear discrete dynamical system.

The unknown impulsive thrust maneuver capability of the vehicle provides a problem to the tracker. The standard Kalman filtering technique is not equipped to handle this problem as it requires knowledge of the entire stochastic and deterministic behavior of the maneuvering thrust of the system. A rapid estimation scheme[4] for linear system and measurement equations was derived to evaluate the state error covariance matrix based upon the measurable and the known quantities when the state change is detected by the observer. In this paper, a rapid estimation scheme is presented for the nonlinear system appearing in this problem.

State Variables of a Thrust Maneuvering Orbit

The motion of a space vehicle above the Earth's atmosphere is essentially a two body problem with six orbital states to be tracked for the determination of an osculating orbit. These six state variables[8] are: the semimajor axis a, the eccentricity e, the eccentric anomaly E, the longitude of the ascending node Ω, the inclination angle i, and the argument of perihelion ω. A new variable is now introduced to assist in the determination of the trajectory following the unknown impulsive thrust maneuvering. This new state is the eccentric anomaly E° of the vehicle at the initial clock measurement time t_o (i.e., the time of vehicle acquisition by ground radar). The value of E° is initially unknown to the observer and changes abruptly to a new value when thrust maneuvering is applied, because the line of apsides of the orbit changes its location for the same time t_0. Therefore, it is necessary to track the quantity E° in addition to the six orbital states for the determination of the trajectory of the maneuvering vehicle. Defining x as the state vector of the problem, i.e.,

$$x_k \triangleq [a_k, e_k, E_k^\circ, E_k, \Omega_k, i_k, \omega_k]^T \quad (1)$$

where the subscript k denotes the quantities at the standard Greenwich clock measurement time t_k.

Position Vector of the Ground Tracking Station

A ground radar tracking station located on Earth has longitude ϕ and latitude λ. The Earth is rotating at a constant angular velocity ω_E (rad/sec). The following is the transformation[9] of the radar station's position vector q_k from Earth's geographical frame to the inertial frame to be defined later

Presented as Paper 71-902 at the AIAA Guidance, Control and Flight Mechanics Conference, Hofstra University, Hempstead, N.Y., August 16–18, 1971; submitted September 9, 1971; revision received January 17, 1972. This research is sponsored by the Department of Defense, under Project Themis Contract DAAB07-69-C-0365. The U.S. Government reserves the right to separately reproduce and distribute published material which results from research under this contact. Part of this paper is submitted to the School of Engineering at Rensselaer Polytechnic Institute as partial fulfilment of the degree of Doctor of Engineering under the above contract at Rensselaer Polytechnic Institute.

Index catagories: Navigation, Control and Guidance Theory; Computer Technology and Computer Simulation Techniques.

* Member of Technical Staff, Mathematical Applications Department, Systems Division.

† Professor of Mechanical Engineering. Member AIAA.

$$q_k^{(\bar{n})} = |q_k^{(\bar{g})}| [-\cos\lambda \sin(\theta_k + \phi), \cos\lambda \cos(\theta_k + \phi), \sin\lambda]^T \quad (2)$$

where the superscript $(\bar{n})$ denotes the vector quantities expressed in an inertial frame which is defined by a right-hand triplet in the direction of the vernal equinox and the Earth's north pole as shown in Fig. 1. The superscript $(\bar{g})$ denotes the vector quantities expressed in the Earth's geographical frame. The angle $\theta_k = \omega_E \cdot t_k$ is the elapsed angle due to Earth's rotation.

Position and Modified Angular Momentum Vectors of the Vehicle

The equation of motion of a free flight vehicle is derived from the two-body problem. A reference frame $(\bar{R})$ is chosen to define the orbital plane in the inertial space as one can see in Fig. 1. The position and modified angular momentum vectors r and α of the vehicle can be expressed[8] in the reference frame $(\bar{R})$ at time t_k as

$$r_k^{(\bar{R})} = [a_k(\cos E_k - e_k), a_k(1-e_k^2)^{1/2} \sin E_k, 0]^T \quad (3)$$

$$\alpha_k^{(\bar{R})} = [-(\mu a_k)^{1/2} \sin E_k, \{\mu a_k(1-e_k^2)\}^{1/2} \cos E_k, 0]^T \quad (4)$$

where μ is the universal gravitational constant of the Earth.

A linear transformation[10] of the position vector $r_k^{(\bar{R})}$ and modified angular momentum vector $\alpha_k^{(\bar{R})}$ from the reference frame $(\bar{R})$ to the chosen inertial frame can be written as

$$r_k^{(\bar{n})} = G_\Omega G_i G_\omega r_k^{(\bar{R})} \quad (5)$$

$$\alpha_k^{(\bar{n})} = G_\Omega G_i G_\omega \alpha_k^{(\bar{R})} \quad (6)$$

where the quantities G_Ω, G_i and G_ω are (3×3) orthogonal Euler rotational matrices.[10]

Measurement Equations

The (3×1) vehicle position vector $\rho_k^{(\bar{g})}$ and the (3×1) modified angular momentum vector $\delta_k^{(\bar{g})}$ are measured from the radar station by range and rate radar.[11] These two measurement vectors can also be transformed into the inertial frame as follows:

$$\begin{aligned} \rho_k^{(\bar{n})} &= A^{-1}(\theta_k) B^{-1}(\phi) N^{-1}(\lambda) \rho_k^{(\bar{g})} \\ \delta_k^{(\bar{n})} &= A^{-1}(\theta_k) B^{-1}(\phi) N^{-1}(\lambda) \delta_k^{(\bar{g})} \end{aligned} \quad (7)$$

where

$$A(\theta_k) \triangleq \begin{bmatrix} \cos\theta_k & \sin\theta_k & 0 \\ -\sin\theta_k & \cos\theta_k & 0 \\ 0 & 0 & 1 \end{bmatrix},$$

$$B(\phi) \triangleq \begin{bmatrix} \cos\phi & \sin\phi & 0 \\ -\sin\phi & \cos\phi & 0 \\ 0 & 0 & 1 \end{bmatrix}, \quad (8)$$

$$N(\lambda) \triangleq \begin{bmatrix} 1 & 0 & 0 \\ 0 & \cos\lambda & -\sin\lambda \\ 0 & \sin\lambda & \cos\lambda \end{bmatrix}$$

Noting that the matrices in Eq. (8) are orthogonal matrices, their inverse are equal to their transpose.

Combining Eqs. (2 and 5–7) and considering the clock time t_k as another measurement quantity, a set of measurement equations can be obtained as

$$z_k = h(x_k) + v_k \quad (9)$$

where the (7×1) measurement vector z_k containing all the known measurement quantities is given as

$$z_k = [\{\rho_k^{(\bar{n})} + q_k^{(\bar{n})}\}, \{\delta_k^{(\bar{n})} + [-\sin(\theta_k+\phi)\sin\lambda, \cos(\theta_k+\phi)\sin\lambda, \cos\lambda]^T \omega_E R_o^2\}, (t_k - t_o)]^T \quad (10a)$$

where R_o is the radius of the Earth. The (7×1) vector function $h(x_k)$ as a function of the seven states is

$$h(x_k) = \begin{bmatrix} G_\Omega G_i G_\omega [a_k(\cos E_k - e_k), a_k(1-e_k^2)^{1/2} \sin E_k, 0]^T \\ G_\Omega G_i G_\omega [-(\mu a_k)^{1/2} \sin E_k, \{\mu a_k(1-e_k^2)\}^{1/2} \cos E_k, 0]^T \\ (a_k^3/\mu)^{1/2} \{(E_k - E_k^\circ) - e_k(\sin E_k - \sin E_k^\circ)\} \end{bmatrix} \quad (10b)$$

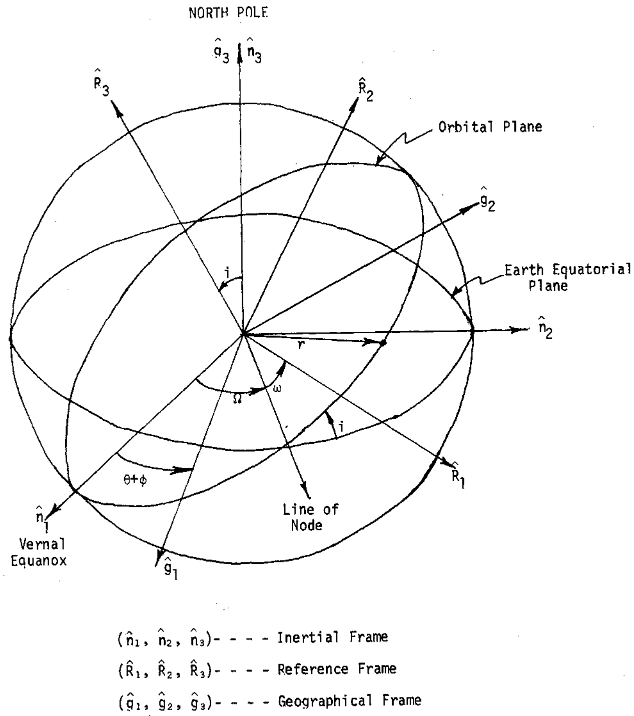

Fig. 1 The coordinate systems.

The (7×1) measurement noise vector v_k is

$$v_k = [A^{-1}(\theta_k) B^{-1}(\phi) N^{-1}(\lambda) u_k^{(\bar{g})}, A^{-1}(\theta_k) B^{-1}(\phi) N^{-1}(\lambda) u_k^{*(\bar{g})}, u_k^t]^T \quad (10c)$$

The quantities $u_k^{(\bar{g})}$ and $u_k^{*(\bar{g})}$ are the actual position and modified angular momentum measurement noise vectors taken along the three axes of the geographical frame and u_k^t is the scalar measurement error of the clock. Equation (9) constitutes a new set of seven nonlinear measurement equations of the vehicle in terms of seven orbital states.

Dynamic Equations

By assuming a Markov process and discretizing the Kepler's equation as shown in Appendix A, a set of nonlinear dynamic equations is obtained to describe the relation of the states before and after the thrust maneuvering with measurement time interval Δt_k as a parameter.[12] That is,

$$x_k = f(x_{k-1}) + w_{k-1} \quad (11)$$

where the (7×1) vector function $f(x_{k-1})$ of the states is

$$f(x_{k-1}) = [a_{k-1}, e_{k-1}, E_{k-1}^\circ, \{E_{k-1} + (\mu/a_{k-1}^3)^{1/2} \Delta t_k / (1 - e_{k-1}\cos E_{k-1})\}, \Omega_{k-1}, i_{k-1}, \omega_{k-1}]^T \quad (12a)$$

and the (7×1) unknown forcing input vector w_{k-1} is

$$w_{k-1} = [w_{k-1}^a, w_{k-1}^e, w_{k-1}^{E^\circ}, w_{k-1}^E, w_{k-1}^\Omega, w_{k-1}^i, w_{k-1}^\omega]^T \quad (12b)$$

The quantity w_{k-1} is zero when no thrust is applied in the arbitrary interval $[k-1, k]$ or the quantity w_{k-1} is the change of states when thrust is applied in the interval $[k-1, k]$ as shown in Appendix A.

Second-Order Filtering Relation for Discrete Nonlinear Processes

A second-order filtering relation is derived for the nonlinear discrete measurement and dynamic relations of Eqs. (9) and (11). The second order filter will yield a better state estimate than the quasilinear filtering technique especially when the measurement interval Δt_k is large.

Estimation Procedure for the System Dynamics

Following the procedure of the section on Measurement Equations, in Ref. 7 by considering a discrete nonlinear dynamical system given by Eq. (11), the following second-order estimation equations for system dynamics can be obtained by assuming an unbiased estimation relation, i.e.,

$$E[x_{k-1}-\hat{x}_{k-1}] \equiv 0, \qquad E[x_k-\bar{x}_k] \equiv 0 \tag{13}$$

where the quantity $\hat{x}_{k-1}$ denotes the best estimate of the state vector x after the $(k-1)$ measurement stage and the quantity $\bar{x}_k$ denotes the best predicted value of x at kth stage before the measurement.

Employing a second-order Taylor's expansion of the function $f(x_{k-1})$ along the known trajectory $\hat{x}_{k-1}$ yields:

$$f(x_{k-1}) \simeq f(\hat{x}_{k-1})+F(\hat{x}_{k-1})(x_{k-1}-\hat{x}_{k-1})+ \frac{1}{2}\sum_{j=1}^{7} \phi_j (x_{k-1}-\hat{x}_{k-1})^T A_j(\hat{x}_{k-1})(x_{k-1}-\hat{x}_{k-1}) \tag{14}$$

where the quantities $\phi_1, \phi_2, \ldots, \phi_j$ denote the (7×1) natural orthonormal basis vectors, and the (7×7) matrices $F(\hat{x}_{k-1})$ and $A_j(\hat{x}_{k-1})$ are defined as

$$F(\hat{x}_{k-1}) \triangleq \left.\frac{\partial f}{\partial x}\right|_{\hat{x}_{k-1}}, \quad A_j(\hat{x}_{k-1}) \triangleq \left.\frac{\partial^2 f^j}{\partial x_p \partial x_q}\right|_{\hat{x}_{k-1}} \quad p,q = 1\ldots 7 \tag{15}$$

where f^j is the jth element in the vector function $f(x_{k-1})$ given in Eq. (12a).

Employing Eqs. (13) and (14), the best prior estimate of the state vector $\bar{x}_k$ can thus be obtained as follows:

$$\bar{x}_k = f(\hat{x}_{k-1})+\bar{w}_{k-1}+\bar{c}_{k-1} \tag{16}$$

where the quantity $\bar{w}_{k-1}$ denotes the mean of the forcing input vector w_{k-1}. The vector $\bar{c}_{k-1}$ which is the bias correction term of the prior estimation due to the second-order correction is found to be

$$\bar{c}_{k-1} = \frac{1}{2}\sum_{j=1}^{7} \phi_j \, tr[A_j(\hat{x}_{k-1})P_{k-1}] \tag{17}$$

where the matrix P_{k-1} is the state error covariance matrix at the $(k-1)$ stage defined as

$$P_{k-1} \triangleq E[(x_{k-1}-\hat{x}_{k-1})(x_{k-1}-\hat{x}_{k-1})^T] \tag{18}$$

Similarly, the relation of updating the state error covariance matrix M_k prior to the kth measurement defined as

$$M_k \triangleq E[(x_k-\bar{x}_k)(x_k-\bar{x}_k)^T] \tag{19}$$

is found to be

$$M_k = F(\hat{x}_{k-1})P_{k-1}F^T(\hat{x}_{k-1})+Q_{k-1}+C_{k-1} \tag{20}$$

where the jith element of the matrix C_{k-1} can be expressed as the following:

$$(C_{k-1})_{ji} = \tfrac{1}{2}\, tr[A_j(\hat{x}_{k-1})P_{k-1}A_i(\hat{x}_{k-1})P_{k-1}] \tag{21a}$$

and the covariance matrix of the forcing input is defined as[12]

$$Q_{k-1} \triangleq E[(w_{k-1}-\bar{w}_{k-1})(w_{k-1}-\bar{w}_{k-1})^T] \tag{21b}$$

Equation (20) gives the second order discrete dynamic relation for the state error covariance matrix estimate prior to the measurement at the kth stage. It is equivalent to Eq. (28) in Ref. 7, which employs a Ricatti equation to solve for the state error covariance matrix for a continuous time dynamical system.

Estimation Procedure After Measurement

The second order filtering relation for the best state estimate utilizing the measurement z_k can be written as

$$\hat{x}_k = \bar{x}_k+K_k[z_k-h(\bar{x}_k)]+\bar{l}_k \tag{22}$$

where K_k is the Kalman gain matrix and the vector $\bar{l}_k$ is the bias correction term of the state estimation corresponding to the kth measurement.

The state vector $\bar{x}_k$ is now available to the tracker. Employing a second-order Taylor's expansion of the vector function $h(x_k)$ along $\bar{x}_k$ and defining $\bar{e}_k$ as the difference between x_k and $\bar{x}_k$ yields

$$h(x_k) \simeq h(\bar{x}_k)+H(\bar{x}_k)\bar{e}_k+\frac{1}{2}\sum_{j=1}^{7}\phi_j \bar{e}_k^T D_j(\bar{x}_k)\bar{e}_k \tag{23}$$

where the (7×7) matrices $H(\bar{x}_k)$ and $D_j(\bar{x}_k)$ are defined as

$$H(\bar{x}_k) \triangleq \left.\frac{\partial h}{\partial x}\right|_{\bar{x}_k}, \quad D_j(\bar{x}_k) \triangleq \left.\frac{\partial^2 h^j}{\partial x_p \partial x_q}\right|_{\bar{x}_k} \quad p,q = 1\ldots 7 \tag{24}$$

and the quantity h^j is the jth element of the vector function $h(x_k)$ given in Eq. (10b).

Employing Eqs. (13, 19, 22, and 23), the relation for the best estimate of the states and the covariance matrix can be written as

$$K_k = M_k H^T(\bar{x}_k)[H(\bar{x}_k)M_k H^T(\bar{x}_k)+R_k+L_k]^{-1} = P_k H^T(\bar{x}_k)R_k^{-1} \tag{25}$$

$$P_k = M_k - M_k H^T(\bar{x}_k)[H(\bar{x}_k)M_k H^T(\bar{x}_k)+R_k+L_k]^{-1}H(\bar{x}_k)M_k \tag{26}$$

$$\hat{x}_k = \bar{x}_k+K_k[z_k-h(\bar{x}_k)]+\bar{l}_k \tag{27}$$

where

$$R_k \triangleq E[v_k v_k^T] \tag{28}$$

$$\bar{l}_k = -\frac{1}{2}K_k\sum_{j=1}^{7}\phi_j \, tr[D_j(\bar{x}_k)M_k] \tag{29}$$

$$(L_k)_{ji} = \tfrac{1}{2}\, tr[D_j(\bar{x}_k)M_k D_i(\bar{x}_k)M_k] \tag{30}$$

The derivations of Eqs. (25–30) are given in Ref. 7 and are not repeated in this paper.

Summary of the Second-Order Discrete Filtering Relations

When tracking an unknown thrust maneuvering space vehicle, neither the magnitude nor the time of impulsive thrusting is known to the tracker. Thus, the knowledge of the quantities $\bar{w}_{k-1}$ and Q_{k-1} are not available, and it is convenient to set these two quantities equal to zero. The second-order discrete filtering relation can be summarized as follows:

$$\begin{gathered}\bar{x}_k = f(\hat{x}_{k-1})+\bar{c}_{k-1}, \quad M_k = F(\hat{x}_{k-1})P_{k-1}F^T(\hat{x}_{k-1})+C_{k-1} \\ P_k = M_k - M_k H^T(\bar{x}_k)[H(\bar{x}_k)M_k H^T(\bar{x}_k)+R_k+L_k]^{-1}H(\bar{x}_k)M_k \\ \hat{x}_k = \bar{x}_k+P_k H^T(\bar{x}_k)R_k^{-1}[z_k-h(\bar{x}_k)]+\bar{l}_k\end{gathered} \tag{31}$$

where the quantities $\bar{c}_{k-1}$, C_{k-1}, $\bar{l}_k$ and L_k are the second-order correction terms given in Eqs. (17, 21a, 29, and 30), respectively. If these terms are set equal to zero, the filtering relations of Eq. (31) reduce to the usual extended Kalman filtering relations for a discrete nonlinear system.[12]

Rapid Estimation Scheme-Evaluation of the Prior State Error Covariance Matrix

Because no knowledge of the thrusting maneuver of the vehicle is given to the tracking station, neither the forcing input vector w_{k-1} nor its covariance matrix Q_{k-1} is available to the observer. The filtering relation given in Eq. (31) will not provide reasonable results following a state jump since it does not include the unknown forcing quantity. A measurable covariance matrix is introduced[4] which provides a corrected prior state error covariance matrix based upon the reliable measurement quantities obtained immediately after the thrust maneuvering.

The (7×7) measurable covariance matrix for the nonlinear processes is defined as

$$U_k \triangleq E\{[z_k-h(\bar{x}_k)]\,[z_k-h(\bar{x}_k)]^T\} \tag{32}$$

Substituting Eq. (9) into Eq. (32) yields

$$U_k = E\{[h(x_k)-h(\bar{x}_k)+v_k][h(x_k)-h(\bar{x}_k)+v_k]^T\} \tag{33}$$

Employing Eq. (23), Eq. (33) becomes

$$U_k = E\left\{\left[H(\bar{x}_k)\bar{e}_k+\frac{1}{2}\sum_{j=1}^{7}\phi_j\bar{e}_k^T D_j(\bar{x}_k)\bar{e}_k+v_k\right]\times \left[\bar{e}_k^T H^T(\bar{x}_k)+\frac{1}{2}\sum_{i=1}^{7}\phi_i^T\bar{e}_k^T D_i(\bar{x}_k)\bar{e}_k+v_k^T\right]\right\} \tag{34}$$

The measurement noise vector v_k is assumed to be zero-mean Gaussian white noise which is uncorrelated to the error vector $\bar{e}_k$. Thus

$$E[v_k] \equiv 0, \qquad E[\bar{e}_k v_k^T] \equiv 0 \tag{35}$$

Employing Eqs. (19, 28, and 35) together with the Lemma given in Ref. 14, Eq. (34) can be written as

$$U_k = H(\bar{x}_k)M_k^{\dagger}H^T(\bar{x}_k) + R_k + S_k \tag{36}$$

where the superscript † denotes that the quantity is evaluated with measureable quantities.

The jith element of the matrix S_k can be written as

$$(S_k)_{ji} = \tfrac{1}{2} tr[D_j(\bar{x}_k)M_k^{\dagger}D_i(\bar{x}_k)M_k^{\dagger}] + \tfrac{1}{4} tr[D_j(\bar{x}_k)M_k^{\dagger}]\, tr[D_i(\bar{x}_k)M_k^{\dagger}] \tag{37}$$

The measurable covariance matrix U_k is based upon the measurement quantity z_k and the prior state estimate vector $\bar{x}_k$. Thus, the matrix U_k can be evaluated at the kth stage with measurement obtained by the tracker.[4] The perturbation matrices $H(\bar{x}_k)$ and $D(\bar{x}_k)$ are evaluated along the known quantity $\bar{x}_k$. The noise covariance matrix R_k depends upon the accuracy of the tracking instruments and is known to the tracker. Thus, Eq. (36) provides a set of 28 equations to solve for the elements of the symmetrical prior state error covariance matrix $M_k^{\dagger}$. Once the correct value of the matrix $M_k^{\dagger}$ is found from Eq. (36), the estimation procedure can be continued with Eqs. (26) and (27) to obtain an improved estimation of the states.

Obtaining the correct matrix $M_k^{\dagger}$ from Eq. (36) is very time consuming for an on-line tracking problem. An approximation can be made to simplify the determination of the matrix $M_k^{\dagger}$ by neglecting the second order expansion terms in Eq. (23), i.e.,

$$h(x_k) \simeq h(\bar{x}_k) + H(\bar{x}_k)\bar{e}_k \tag{38}$$

Utilizing the approximation of Eq. (38) to compute the approximation of Eq. (36) the relation between the matrices U_k and $M_k^{\dagger}$ can be written as

$$U_k = H(\bar{x}_k)M_k^{\dagger}H^T(\bar{x}_k) + R_k \tag{39}$$

If the (7×7) matrix $H(\bar{x}_k)$ is nonsingular, Eq. (39) can be written as

$$M_k^{\dagger} = H^{-1}(\bar{x}_k)(U_k - R_k)H^{-T}(\bar{x}_k) \tag{40}$$

Eq. (40) provides an explicit relation to determine the prior state error covariance matrix $M_k^{\dagger}$ from the dependable measurable covariance matrix U_k employing a first order approximation of the function $h(x_k)$. By comparing Eqs. (36) and (39) it is evident that the only difference is the second-order correction matrix S_k. Although some accuracy is lost by employing Eq. (40) to find the matrix $M_k^{\dagger}$, the computation time for Eq. (40) is much shorter than solving explicitly the 28 nonlinear equations given by Eq. (36). Notice that Eq. (39) is equivalent to Eq. (27) in Ref. 4 for a linear process.

The reason that Eq. (39) will provide a better value of the prior state error covariance matrix $M_k^{\dagger}$ when unknown impulsive thrusting is applied is shown in Appendix B. The following relation summarizes the rapid estimation procedure immediately following a state jump.

$$\bar{x}_k = f(\hat{x}_{k-1}) + \bar{c}_{k-1}, \quad M_k^{\dagger} = H^{-1}(\bar{x}_k)(U_k - R_k)H^{-T}(\bar{x}_k)$$
$$P_k^{\dagger} = M_k^{\dagger} - M_k^{\dagger}H^T(\bar{x}_k)[H(\bar{x}_k)M_k^{\dagger}H^T(\bar{x}_k) + R_k + L_k]^{-1}H(\bar{x}_k)M_k^{\dagger}$$
$$\hat{x}_k = \bar{x}_k + P_k H^T(\bar{x}_k)R_k^{-1}[z_k - h(\bar{x}_k)] + \bar{l}_k \tag{41}$$

The rapid estimation procedure given in Eq. (41) does not require a direct inversion of the ill-condition matrix U_k as in the rapid estimation scheme in Ref. 4.

Detecting the Instant of Impulsive Thrusting

The estimation procedure given in Eq. (41) gives a proper estimation of the state because the correct prior state error covariance matrix $M_k^{\dagger}$ is found after the unknown thrusting is applied. However, Eq. (31) gives a suboptimal state estimation when no thrusting is applied by carrying the stochastic continuity of the covariance matrices. Therefore, it is suggested that the new evaluation of matrix $M_k^{\dagger}$ is employed only immediately following an unknown thrusting by the vehicle. Because of this consideration, it becomes vitally important to detect the instant of the thrust maneuvering so that the observer can determine which estimation scheme is to be employed.

A detection scheme has been devised[4] based on the characteristics of the matrices U_k and R_k by assigning a parameter β in the following definition:

$$\text{DR.} = \text{Detection Ratio} \triangleq tr \cdot U_k / tr \cdot R_k \geqq \beta \tag{42}$$

When Eq. (42) is satisfied, it is assumed that the thrusting has occurred and Eq. (40) is employed to find the proper matrix $M_k^{\dagger}$. When DR. is less than β, the system is taken to be unforced thus the recursive second-order discrete filtering relation given in Eq. (31) is used to provide the suboptimal state estimation.

The determination of the magnitude of the parameter requires some further research. It is found that: 1) the detection ratio is always a positive valued function of the physical constraints of the maneuvering thrust energy level. 2) The detection ratio decreases as the measurement noise level increases. Thus, if the unknown input is assumed to be founded in a certain region due to the physical constraints of the system, or an energy bound for the impulsive thrusting maneuverability is assumed, then the values of β can be found to satisfy the detection.

Numerical Results

a. Reference Trajectory

In order to illustrate the on-line tracking problem of a thrust maneuvering vehicle, a reference trajectory is assigned. After acquisition by the ground station, the vehicle initially travels along an elliptic Earth orbit for 10 min., then it converts to a lower altitude elliptic orbit with an impulsive thrusting. Following the thrusting maneuver, the orientation of the orbit is altered with the argument of perihelion ω changing from 15° to 24° 11′. The reference values of the orbital states immediately before and after thrusting are shown in Table 1. One can visualize from the table that the quantity E° changes from 15° to a completely new value of 8° 14′ due to the thrusting.

The seven measurement quantities at each stage are calculated from Eq. (10b). A double precision random number subroutine[15] generating normal deviates for a Gaussian distribution with zero mean and unit standard deviation is employed to provide the random additive noise to the measurements given in Eq. (10c). Different noise levels for each measurement are obtained by the assignment of different percent standard deviates from σ^1 to σ^7, corresponding to the seven measurement quantities.

b. Starting Algorithm

In order to employ Eq. (31) for the state estimation, the a priori values of the state vector $\hat{x}_o$ and its error covariance matrix P_o are required to start the recursive estimation process. For a linear system, one can always initialize the problem by employing a least square filtering procedure once the first set of measurement data is available.[4] For a nonlinear system, if those two values are not available, the observer must guess an initial state vector $\hat{x}_o$ and use some curve fitting or smoothing technique to find the proper state error covariance matrix P_o. These processes may be cumbersome and time consuming in the on-line estimation problem. A new starting method is suggested that employs the guessed value of $\hat{x}_o$. The difference between

Table 1 State variables before and after the impulsive thrusting R_o = Earth radius = 3963.2 miles

Orbital states		Orbit (1)	Orbit (2)	Change
Semimajor axis	a	$1.5R_o$	$1.65R_o$	$0.15R_o$
Eccentricity	e	0.30	0.35	0.05
Initial eccentric anomaly	E°	15°	8° 14′	−6° 46′
Eccentric anomaly	E	46° 20′	36° 50′	−9° 30′
Longitude of ascending node	Ω	45°	45°	0
Inclination angle	i	30°	30°	0
Argument of perihelion	ω	15°	24° 11′	9° 11′

this guessed value of $\hat{x}_o$ and its actual value x_o can be treated as a jump in the value of the state vector. The algorithm for this suggested starting procedure is listed as follows: 1) guess an $\hat{x}_o$, 2) let $\bar{x}_1 = f(\hat{x}_o)$, 3) after the measurement vector z_1 is obtained by the observer, evaluate the matrix U_1 and $H(\bar{x}_1)$, 4) employ Eq. (40) to obtain $M_1^{\dagger}$, 5) use $\bar{x}_1$ and $M_1^{\dagger}$ to initiate the recursive estimation process given in Eq. (31). It is found that the above starting algorithm for the filtering process provides a correct state estimate.

c. Simulation Results

For the assigned reference trajectory, four different estimation schemes are implemented on a digital computer. First, only the quasilinear filtering technique is employed throughout the entire process. Second, the second order filtering relation described by Eq. (31) is used for the entire process. Third, the quasilinear filter is combined with the rapid estimation scheme, and finally, the second order filtering is combined with the rapid estimation scheme. In each of these last two cases the rapid estimation scheme is utilized only when the state jump is detected from Eq. (42). The algorithm described in part (b) is employed for all four experiments in order to provide the proper starting of the estimation process. Different time intervals $\Delta t_k = 15$, 30, and 60 sec are used for each different method. In order to save computation time for an on-line problem and emphasize the importance of the dynamical relation, only the correction terms $\bar{c}_{k-1}$ and C_{k-1} in Eq. (31) are considered for the second-order filter while the terms from the measurement correction $\bar{l}_k$ and L_k are eliminated from the estimation process. The percent standard deviations of the measurement σ^1 to σ^6 are taken to be 0.01 and σ^7 is taken to be 0.0001 due to the more accurate clock measurement. The detection ratio DR is plotted vs time as shown in Fig. 2. One can visualize from Fig. 2 that the value of the detection ratio DR jumps abruptly when a state jump occurs. The parameter value of $\beta = 10$ is assigned to perform the proper detection. This chosen value of β is lower than the value of DR at the instant of the state jump but is higher than its value produced by the largest measurement noise. If the value of β is chosen to be too high, no maneuver thrusting of the vehicle will be detected and the unforced estimation procedure will be employed throughout the entire process. A poor estimate of the state variable will result after the impulsive thrust maneuvering. If the value of β is chosen to be too low, false jump will result in the detecting scheme. The rapid estimation scheme will be applied several times when there is no state jump. The development of a more discriminating detection scheme is currently the topic of further research. Figures 3–5 show the absolute value of the errors between the reference values given in Table 1 and the estimated values of the state variables a, e and ω, for a measurement time interval $\Delta t_k = 15$ sec. Figures 6, 7 and 8 show the errors for these same state variables for a measurement time interval $\Delta t_k = 60$ sec. One can visualize from Figs. 3–8 that the first two estimation procedures listed above do not provide the proper state estimate after the abrupt change of states. On the other hand, the estimation scheme which includes rapid estimation reduces the error immediately after the state jump. The

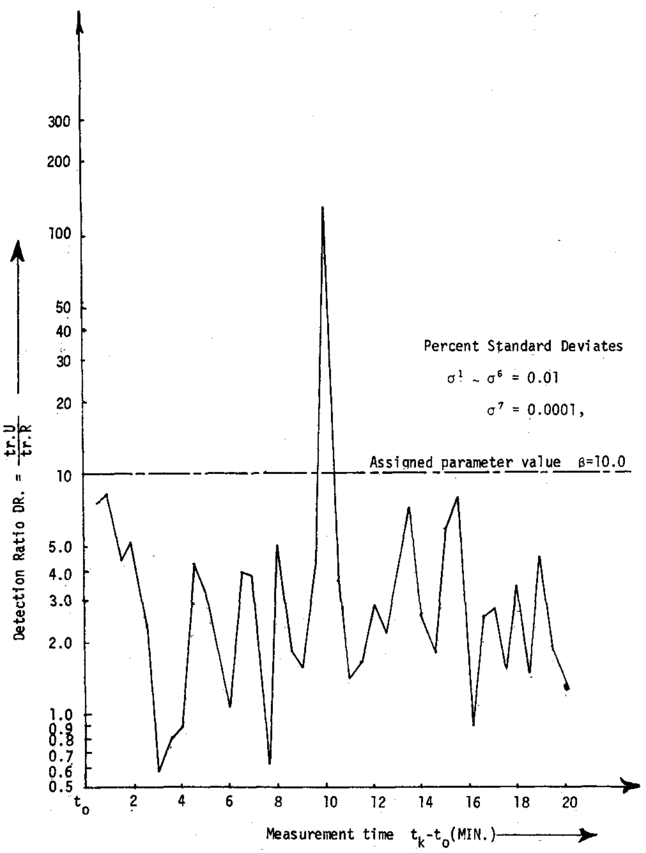

Fig. 2 Detection ratio DR vs measurement time with $\Delta t_k = 30$ sec.

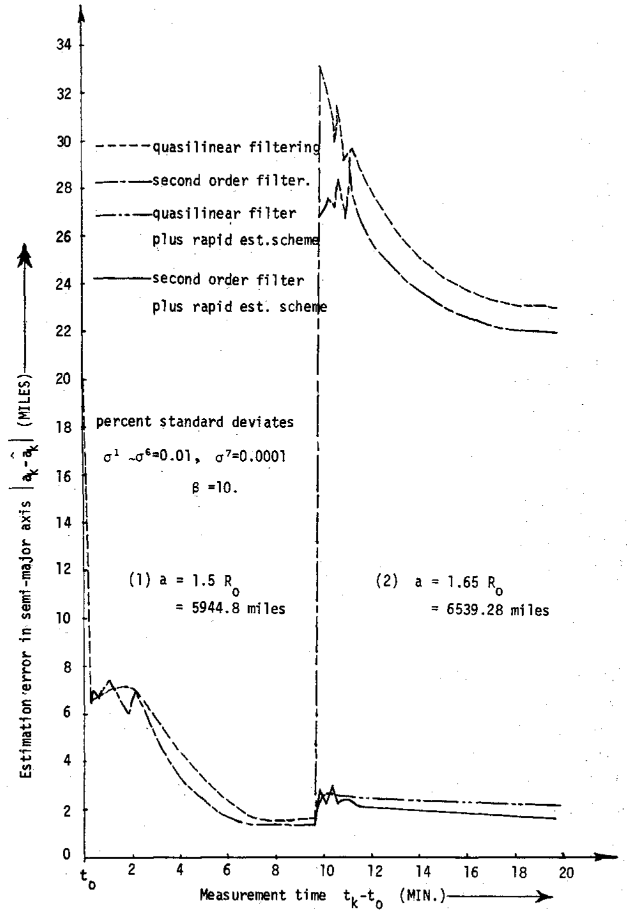

Fig. 3 Estimation error in semimajor axis a with $\Delta t_k = 15$ sec.

Table 2 Estimation errors in semimajor axis a for different time intervals

Measurement time interval Δt_k, sec	Estimation error immediately before thrusting, miles		Smallest estimation error after thrusting, miles			
	Method[a] (1)	Method[a] (2)	Methods[a] (1)	(2)	(3)	(4)
15	1.586	1.397	22.852	21.755	2.198	1.803
30	2.120	1.779	25.263	22.913	2.380	1.998
60	3.412	2.387	30.013	25.327	3.011	2.406

[a] Method (1)—quasilinear filtering; method (2)—second-order filtering; method (3)—quasilinear filter plus rapid est. scheme; method (4)—second-order filter plus rapid est. scheme.

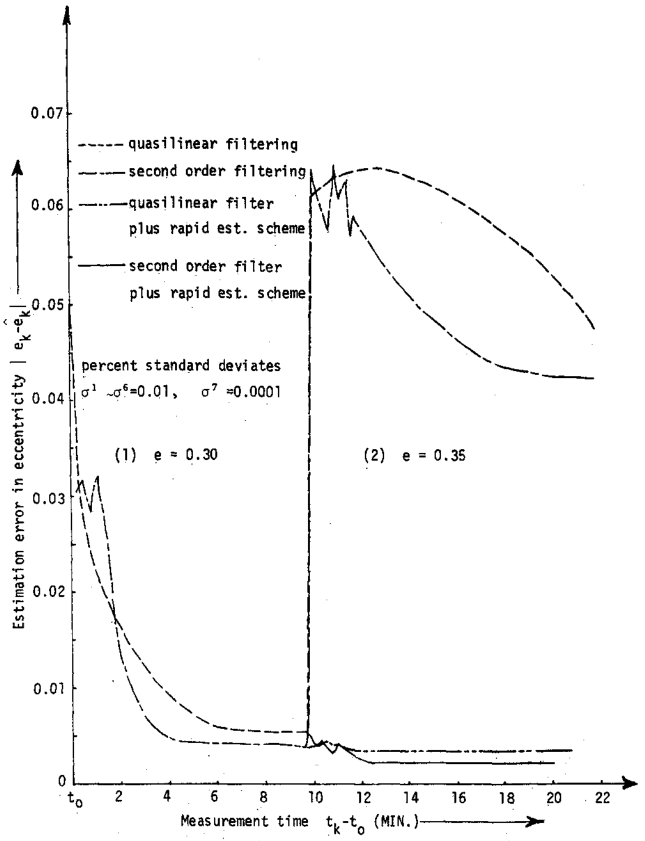

Fig. 4 Estimation error in eccentricity e with $\Delta t_k = 15$ sec.

estimation errors of the semimajor axis a, immediately before the thrusting and the smallest error after the thrusting, is shown in Table 2 for $\Delta t_k = 15$, 30, and 60 sec. One can see from Table 2 that the estimation error for the fourth estimation scheme when

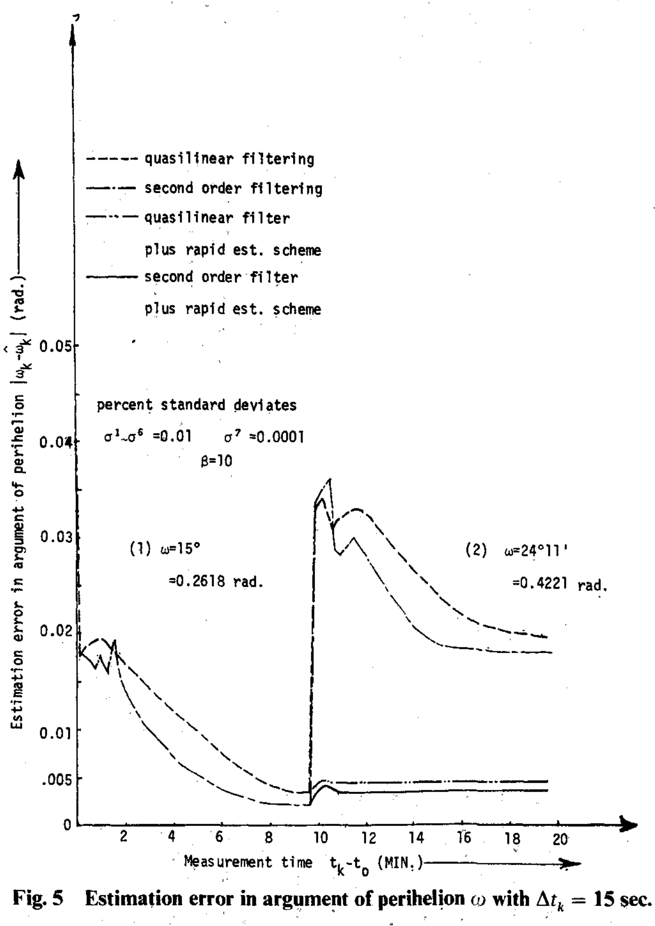

Fig. 5 Estimation error in argument of perihelion ω with $\Delta t_k = 15$ sec.

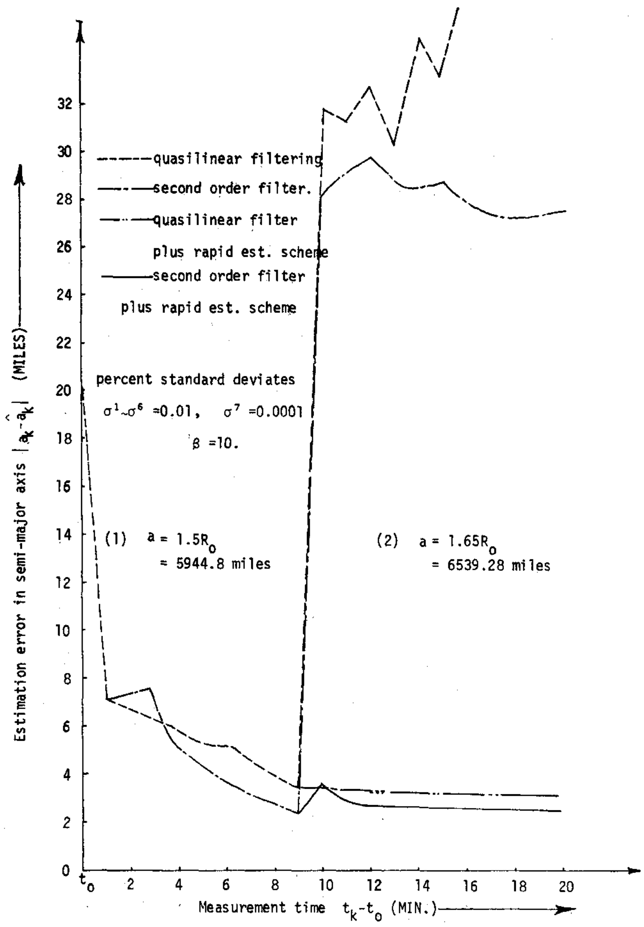

Fig. 6 Estimation error in semimajor axis a with $\Delta t_k = 60$ sec.

$\Delta t_k = 15$ sec is only 7.8% of the error in the first estimation procedure after the thrusting. A considerable improvement is achieved due to the use of a second-order filtering technique together with the rapid estimation scheme. One can see also that the effectiveness of the second order estimation technique is not very significant when compared to quasilinear filter for small measurement time interval, but the second-order filter provides a better improvement when Δt_k is large. For instance, the improvement of the estimation error after the thrusting between method 4 and method 3 is 0.605 miles, between method 4 and method 1 is 27.607 miles for $\Delta t_k = 60$ sec. On the other hand, when Δt_k is reduced to 15 sec, the improvement between method 4 and method 3 is only 0.395 miles, and 21.049 miles between method 4 and method 1. Comparing method 4 for $\Delta t_k = 60$ sec to method 3 for $\Delta t_k = 15$ sec in Table 2, it is also evident that if the tracker must take the large measurement time interval, then the second-order filter can be employed without losing too much accuracy for the state estimation. The utilization of second-order filtering technique also provides the faster convergence of the state estimation and smaller estimation error especially when Δt_k is large as one can see in Figs. 6–8. Similar results are obtained for the estimation of the other state variables.

Conclusion

The problem of on-line tracking of the state variables of a thrust maneuvering space vehicle in three dimensional space described by nonlinear discrete dynamic and measurement equations is studied for several different estimation schemes. A second-order filtering relation is derived for a discrete nonlinear plant which adds bias correction terms to the quasilinear filter. The rapid estimation scheme for a nonlinear system is employed both to provide the starting algorithm and whenever the state jump is detected. The digital computer evaluation indicates that the estimates of the states by the combination of a second-order filter with the rapid estimation scheme is superior to the results

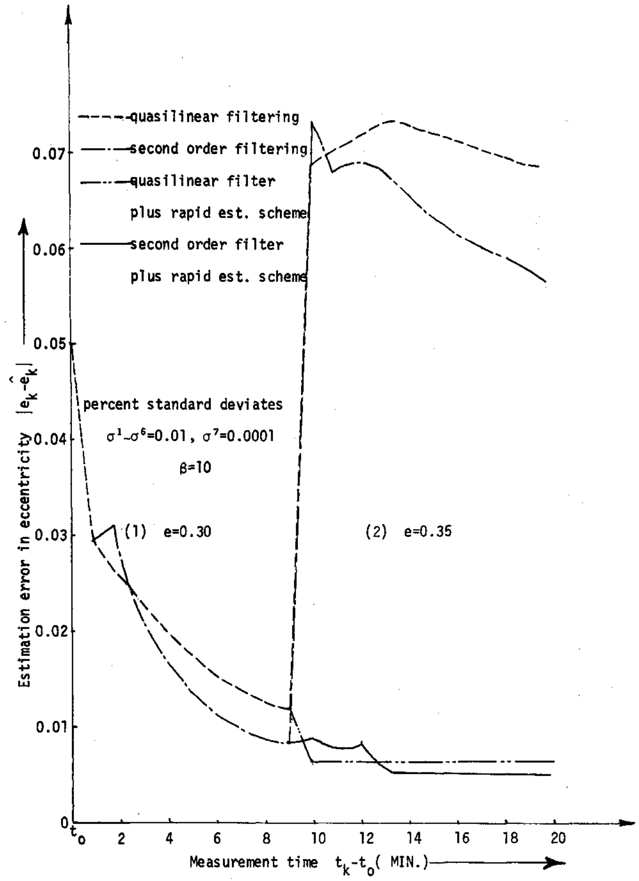

Fig. 7 Estimation error in eccentricity e with $\Delta t_k = 60$ sec.

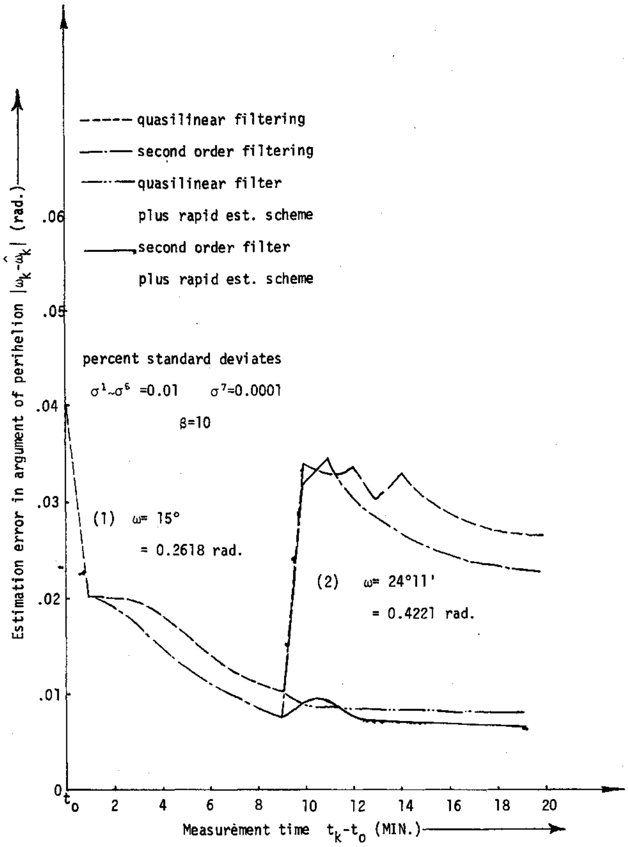

Fig. 8 Estimation error in argument of perihelion ω with $\Delta t_k = 60$ sec.

obtained from quasilinear filtering techniques for the application of tracking the thrust maneuvering space vehicle.

Appendix A

Derivation of the Dynamic Equations

The Kepler's equation can be written as

$$F(a,e,E^\circ,E,t) \triangleq E-E^\circ-e(\sin E-\sin E^\circ)-(\mu/a^3)^{1/2}(t-t_o) \equiv 0 \quad \text{(A1)}$$

Taking the total derivative of Eq. (A1) yields

$$dF = (\partial F/\partial a)\,da+(\partial F/\partial e)\,de+(\partial F/\partial E^\circ)\,dE^\circ+(\partial F/\partial E)\,dE+(\partial F/\partial t)\,dt = 0 \quad \text{(A2)}$$

where all the partial derivatives are to be evaluated along some reference trajectory. The derivatives of the states can be approximated as

$$da \simeq \Delta a_k = a_k-a_{k-1}, \quad dE \simeq \Delta E_k = E_k-E_{k-1}, \quad dt \simeq \Delta t_k = t_k-t_{k-1} \quad \text{etc.} \quad \text{(A3)}$$

Evaluating the partial derivatives from Eq. (A1) at $(k-1)$ stage quantity values and employing the relations given in Eq. (A3), Eq. (A2) becomes

$$\tfrac{3}{2}(\mu/a_{k-1}^5)^{1/2}(t_{k-1}-t_o)\Delta a_k-(\sin E_{k-1}-\sin E_{k-1}^\circ)\Delta e_k+(e_{k-1}\cos E_{k-1}^\circ-1)\Delta E_k^\circ+(1-e_{k-1}\cos E_{k-1})\Delta E_k-(\mu/a_{k-1}^3)^{1/2}\Delta t_k = 0 \quad \text{(A4)}$$

When no impulsive thrust is applied between the time interval $[t_{k-1},t_k]$ the quantities a, e, and E° do not change values, i.e.,

$$a_k = a_{k-1}, \quad e_k = e_{k-1}, \quad E_k^\circ = E_{k-1}^\circ \quad \text{(A5)}$$

Employing Eqs. (A3) and (A5), Eq. (A4) finally becomes

$$E_k = E_{k-1}+(\mu/a_{k-1}^3)^{1/2}\,\Delta t_k/(1-e_{k-1}\cos E_{k-1}) \quad \text{(A6)}$$

When the impulsive thrust is applied in the time interval (t_{k-1},t_k), the states will change abruptly due to the thrusting. Therefore, the forcing elements w_{k-1}^a, w_{k-1}^e, and $w_{k-1}^{E^\circ}$ in Eq. (12b) can be written as

$$w_{k-1}^a \triangleq \Delta a_k, \quad w_{k-1}^e = \Delta e_k, \quad w_{k-1}^E = \Delta E_k^0 \quad \text{etc.} \quad \text{(A7)}$$

Substituting Eq. (A7) into Eq. (A4) and rearranging the equation yields

$$E_k = E_{k-1}+(\mu/a_{k-1}^3)^{1/2}\,\Delta t_k/(1-e_{k-1}\cos E_{k-1})+w_{k-1}^E \quad \text{(A8)}$$

where

$$w_{k-1}^E = f(w_{k-1}^a, w_{k-1}^e, w_{k-1}^E, t_{k-1}-t_o) \quad \text{(A9)}$$

Combining Eqs. (A5, A6, and A8) together with three other state variables Ω, i and ω, the state dynamic equations can thus be written as shown in Eqs. (11, 12a, and 12b).

Appendix B

Relation Between the Matrix $M_k^\dagger$ and the Unknown Forcing Input

Employing Eq. (33) and considering only the first order expansion of the vector function $h(x_k)$, the following relation is obtained

$$U_k = E\{[H(\bar{x}_k)(x_k-\bar{x}_k)+v_k][H(\bar{x}_k)(x_k-\bar{x}_k)+v_k]^T\} \quad \text{(B1)}$$

When the thrusting is applied in the interval $[k-1,k]$, the true value of the state vector x_k is

$$x_k = f(x_{k-1})+w_{k-1} \quad \text{(B2)}$$

The prior state estimate x_k always follows the relation

$$\bar{x}_k = f(\hat{x}_{k-1})+\bar{c}_{k-1} \quad \text{(B3)}$$

Employing Eqs. (14, 17, B2, and B3), Eq. (B1) becomes

$$U_k = E\left\langle\left\{H(\bar{x}_k)\left[F(\hat{x}_{k-1})\hat{e}_{k-1}+\frac{1}{2}\sum_{j=1}^{7}\phi_j\, tr[A_j(\hat{x}_{k-1})(\hat{e}_{k-1}\hat{e}_{k-1}^T-P_{k-1})]+w_{k-1}\right]+v_k\right\}\times\left\{\left[F(\hat{x}_{k-1})\hat{e}_{k-1}+\frac{1}{2}\sum_{i=1}^{7}\phi_i\, tr[A_i(\hat{x}_{k-1})(\hat{e}_{k-1}\hat{e}_{k-1}^T-P_{k-1})]+w_{k-1}\right]^T H^T(\bar{x}_k)+v_k^T\right\}\right\rangle \quad \text{(B4)}$$

Employing the lemma given in Ref. 14 and defining

$$Q_{k-1}{}^{\dagger} \triangleq E[w_{k-1} w_{k-1}{}^{T}] \tag{B5}$$

Eq. (B4) becomes

$$U_k = H(\bar{x}_k)[F(\hat{x}_{k-1})P_{k-1}F^T(\hat{x}_{k-1}) + Q_{k-1}{}^{\dagger} + C_{k-1}]H^T(\bar{x}_k) + R_k \tag{B6}$$

Comparing Eqs. (39) and (B6) yields

$$M_k{}^{\dagger} = F(\hat{x}_{k-1})P_{k-1}F^T(\hat{x}_{k-1}) + C_{k-1} + Q_{k-1}{}^{\dagger} \tag{B7}$$

Comparing Eq. (B7) to the unforced second-order filtering relation given in Eq. (31), one can see that the prior state error covariance matrix $M_k{}^{\dagger}$ contains the forcing matrix $Q_{k-1}{}^{\dagger}$ while in Eq. (31) the forcing matrix is missing. One may observe that if the same state estimate value of $\hat{x}_{k-1}$ is used for both methods, when the unknown thrusting is applied in the interval $[k-1, k]$, the rapid estimation scheme provides the correct state error covariance matrix while the second order filtering relation given in Eq. (31) provides an inaccurate estimate due to the presence of the unknown thrusting.

References

[1] Swerling, P., "First Error Propagation in a Stagewise Smoothing Procedure for Satellite Observations," *Journal of the Astronautical Science*, Vol. 6, 1959, pp. 46–52.

[2] Gunckel, T. L., "Orbit Determination Using Kalman Method," *Proceedings of the Franklin Institute, Navigation*, Vol. 10(3), 1963, pp. 213–291.

[3] Rauch, H. E., "Optimum Estimation of Satellite Trajectories Including Random Fluctuations in Drag," *AIAA Journal*, Vol. 3, No. 4, April 1965, pp. 717–722.

[4] Shen, C. N., "Rapid Estimation of Covariance Matrices for Maneuvering Space Vehicle," AIAA Paper 70-1017, New York, 1970.

[5] Mowery, V. O., "Least Squares Recursive Differential Correction Estimation in Nonlinear Problems," *IEEE Transactions on Automatic Control*, Vol. AC-9, Oct. 1965, pp. 399–407.

[6] Kushner, H. J., "Dynamical Equations for Optimum Nonlinear Filtering," *Journal of Differential Equations*, Vol. 3, April 1967, pp. 179–190.

[7] Athans, M., Wishner, R. P., and Bertolini, A., "Suboptimal State Estimation for Continuous-Time Nonlinear System from Discrete Noisy Measurements," *IEEE Transactions on Automatic Control*, Vol. AC-13, No. 5, Oct. 1968, pp. 504–514.

[8] Battin, R., *Astronautical Guidance*, McGraw-Hill, New York, 1963.

[9] McClure, *Theory of Inertial Guidance*, McGraw-Hill, New York, 1961.

[10] Escobal, *Methods of Orbit Determination*, Wiley, New York, 1965.

[11] Mitchell, R. T., Reynolds, G. W., and Wang, S. K., "Use of Doppler Data to Monitor Space Craft Maneuvers," *JPL Space Programs Summary 37-57*, Vol. 11, 1970.

[12] Bryson, A. E. and Ho., Y. C., *Applied Optimal Control*, Ginn-Blaisdell, Waltham, Mass., 1969, Chap. 12.

[13] Sorenson, H. W., "Kalman Filtering Technique," *Advances on Control Systems*, edited by T. C. Leondes, Academic Press, New York, Vol. 3, A.C. 1966, pp. 219–292.

[14] Athans, M., Wishner, R. P., and Bertolini, A., "Suboptimal State Estimation for Continuous-Time Nonlinear Systems for Discrete Noisy Measurements," JACC Preprint, Ann Arbor, Mich., 1968, pp. 364–377.

[15] *IBM System-360 Programmer's Manual*, Scientific subroutine package, IBM (360A-CM-03X) version III, Feb. 1969.

JUNE 1972 AIAA JOURNAL VOL. 10, NO. 6

An Analytical Model for Nitric Oxide Formation in a Gas Turbine Combustor

RICHARD ROBERTS,* LEONARD D. ACETO,† REINER KOLLRACK,‡ DONALD P. TEIXEIRA,§ AND JOHN M. BONNELL¶
Pratt and Whitney Aircraft Division, United Aircraft Corporation, East Hartford, Conn.

An analytical model has been developed for predicting the influence of combustor geometry and operating conditions on nitric oxide emissions. The principal elements of the analysis are a three-zone internal flowfield model, a fuel droplet burning model incorporating either equilibrium or kinetic rate-limited hydrocarbon thermochemistry, and a treatment of the kinetics of nitric oxide formation. The postulated controlling mechanisms are incorporated using a numerical integration procedure coupled to the combustor flowfield. It is concluded that the assumption of equilibrium hydrocarbon chemistry is adequate for predicting nitric oxide concentration. Parametric results are presented indicating the influence of variation in primary zone equivalence ratio, combustor residence time, and initial fuel droplet size. The influence of a particular combustor modification is directly relatable to changes in the vapor-phase fuel-air distribution within the combustor.

Presented as Paper 71-715 at the AIAA/SAE 7th Propulsion Joint Specialist Conference, Salt Lake City, Utah, June 14–18, 1971; submitted August 7, 1971; revision received January 27, 1972. The authors wish to acknowledge the assistance of B. C. Schlein.

Index categories: Combustion in Heterogeneous Media; Combustion in Gases; Reactive Flows.

* Assistant Project Engineer, Combustion T & R Group. Member AIAA.

† Assistant Project Engineer, Scientific Analysis Group. Member AIAA.

‡ Associate Research Scientist, Scientific Analysis Group.

§ Analytical Engineer, Combustion T & R Group; presently with Southern California Edison Company, Los Angeles, California.

¶ Senior Assistant Project Engineer, Combustion T & R Group. Member AIAA.

Nomenclature

A_{sw} = swirler flow area
C_D = fuel droplet drag coefficient
C_{pg} = specific heat of ambient gas
C_{vsw} = swirler discharge coefficient
D = fuel droplet diameter
g = air mass flow rate through first combustion hole row
i = stoichiometric oxygen-fuel weight ratio
j = fraction of air upstream of the combustion holes entering the recirculation zone (referred to g)
k = fraction of combustion hole air entering the recirculation zone (referred to g)
K_i = ratio of one way equilibrium rate to net reaction rate
k_i = reaction rate constant
L = heat of vaporization of the fuel